ADVANCED FUNCTIONAL MATERIALS
www.afm-journal.de

Viromimetic STING Agonist-Loaded Hollow Polymeric Nanoparticles for Safe and Effective Vaccination against Middle East Respiratory Syndrome Coronavirus

Leon Chien-Wei Lin, Chen-Yu Huang, Bing-Yu Yao, Jung-Chen Lin, Anurodh Agrawal, Abdullah Algaissi, Bi-Hung Peng, Yu-Han Liu, Ping-Han Huang, Rong-Huay Juang, Yuan-Chih Chang, Chien-Te Tseng, Hui-Wen Chen,* and Che-Ming Jack Hu**

The continued threat of emerging, highly lethal infectious pathogens such as Middle East respiratory syndrome coronavirus (MERS-CoV) calls for the development of novel vaccine technology that offers safe and effective prophylactic measures. Here, a novel nanoparticle vaccine is developed to deliver subunit viral antigens and STING agonists in a virus-like fashion. STING agonists are first encapsulated into capsid-like hollow polymeric nanoparticles, which show multiple favorable attributes, including a pH-responsive release profile, prominent local immune activation, and reduced systemic reactogenicity. Upon subsequent antigen conjugation, the nanoparticles carry morphological semblance to native virions and facilitate codelivery of antigens and STING agonists to draining lymph nodes and immune cells for immune potentiation. Nanoparticle vaccine effectiveness is supported by the elicitation of potent neutralization antibody and antigen-specific T cell responses in mice immunized with a MERS-CoV nanoparticle vaccine candidate. Using a MERS-CoV-permissive transgenic mouse model, it is shown that mice immunized with this nanoparticle-based MERS-CoV vaccine are protected against a lethal challenge of MERS-CoV without triggering undesirable eosinophilic immunopathology. Together, the biocompatible hollow nanoparticle described herein provides an excellent strategy for delivering both subunit vaccine candidates and novel adjuvants, enabling accelerated development of effective and safe vaccines against emerging viral pathogens.

1. Introduction

Amidst the growing need for better vaccine technology against emerging infectious threats, antigen and adjuvant delivery by synthetic nanoparticles has shown much promise toward improving vaccine safety and effectiveness.[1] Particulate vaccines have been engineered with virus-mimicking features—including nanoscale morphology,[2] multivalent antigen display,[3] and antigen/adjuvant colocalization[4]—to promote immune cell engagement and antigen processing. However, reliable coupling of antigen and danger signals in a virus-like fashion remains challenging at the nanoscale as the task demands stable adjuvant compartmentalization in functionalizable nanocarriers for antigen association. We herein demonstrate a viral capsid-like hollow polymeric nanoparticle encapsulating an emerging class of STING (stimulator of interferon genes) agonist adjuvant as a viromimetic vaccine platform. Consisting of a thin shell of poly(lactic-*co*-glycolic

Dr. L. C.-W. Lin, B.-Y. Yao, Dr. J.-C. Lin, Dr. Y.-H. Liu, Dr. C.-M. J. Hu
Institute of Biomedical Sciences
Academia Sinica
Taipei 11529, Taiwan
E-mail: chu@ibms.sinica.edu.tw

C.-Y. Huang, Dr. P.-H. Huang, Prof. H.-W. Chen
Department of Veterinary Medicine
National Taiwan University
Taipei 10617, Taiwan
E-mail: winnichen@ntu.edu.tw

Dr. A. Agrawal, A. Algaissi, Prof. C.-T. Tseng
Department of Microbiology and Immunology
The University of Texas Medical Branch
Galveston, TX 77555, USA
E-mail: sktseng@utmb.edu

The ORCID identification number(s) for the author(s) of this article can be found under https://doi.org/10.1002/adfm.201807616.

DOI: 10.1002/adfm.201807616

A. Algaissi
Department of Medical Laboratories Technology
Jazan University
Jazan 45142, Saudi Arabia

Prof. B.-H. Peng
Department of Neurosciences, Cell Biology & Anatomy
The University of Texas Medical Branch
Galveston, TX 77555, USA

Prof. R.-H. Juang
Department of Biochemical Science and Technology
National Taiwan University
Taipei 10617, Taiwan

Dr. Y.-C. Chang
Institute of Cellular and Organismic Biology
Academia Sinica
Taipei 11529, Taiwan

Prof. C.-T. Tseng
Center for Biodefense and Emerging Disease
The University of Texas Medical Branch
Galveston, TX 77555, USA

acid) (PLGA) with a large aqueous core, the hollow nanoparticles stably entrap the soluble adjuvant for antigen conjugation and storage. Owing to the acid-sensitive PLGA hydrolysis, the nanoparticles readily release the adjuvant upon cellular uptake, facilitating immune activation and antigen recognition. To our knowledge, the present work is the first report of a PLGA-based hollow nanocarrier capable of adjustable encapsulation and controlled release of STING agonists for vaccine development.

Localized at the endoplasmic reticulum, STING is a potent inducer of type I interferons (IFNs) typically activated upon intracellular infection.[5] Following stimulation by cytosolic cyclic dinucleotides (CDNs), STING activates IRF3 and NFκB, which in turn upregulate the expression of type I IFNs and other pro-inflammatory cytokines to shape the adaptive immunity.[5b,6] The well-defined immune activation mechanism of CDNs has made them a desirable adjuvant candidate for improving vaccine potency. However, free CDNs are not readily membrane-permeable, and their systemic distribution may trigger undesirable reactogenic effects.[7] In addition, given that type I IFNs are pleiotropic and can undermine immune responses upon out-of-sequence antigen presentation,[8] CDN delivery is preferably synchronized with target antigens for optimal immune potentiation. While multiple formulations have been prepared for CDN delivery,[9] their shortcomings ranging from poor encapsulation efficiency, size limitation, and carrier instability leave much room for carrier improvement. In light of these considerations, we demonstrated that the hollow polymeric nanoparticles can encapsulate tunable levels of cdGMP at a high efficiency and improve the compound's potency and safety. Surface functionalization of the nanoparticles was mediated by incorporation of DSPE-PEG-maleimide in the polymeric shell, which allowed for further antigen conjugation for vaccine preparations (**Figure 1**A). In the present study, a vaccine against Middle East respiratory syndrome coronavirus (MERS-CoV) was prepared based on the viromimetic design.

MERS-CoV is a high-mortality pathogen with an urgent need for effective countermeasures.[10] Since its first isolation from a fatal Saudi patient in 2012, there has been continuous outbreaks with more than 2000 reported cases across 27 countries and a mortality rate of 35%. The *β*-coronavirus is closely related to severe acute respiratory syndrome coronavirus (SARS-CoV), with dromedary camels as the primary reservoir host for human infection.[11] Currently, no effective therapeutic or prophylactic measure is available against the disease, and MERS-CoV vaccine development remains a global health priority identified by the World Health Organization (WHO). While several virus-based vaccines have been explored,[12] major efforts on MERS-CoV vaccine research are devoted to subunit candidates such as MERS-CoV spike protein and its derivatives, S1 protein and receptor binding domain (RBD) for safety and logistical considerations.[13] Ongoing challenges remain, however, as observation of vaccination-induced pulmonary immunopathology in immunized and challenged hosts raises concerns over the use of traditional, Th2-dominant adjuvants.[14] In addition, with cellular immunity being an increasingly recognized component alongside neutralizing antibodies for durable protection against the mutation-prone virus,[15] MERS-CoV vaccines may benefit from technologies that can effectively promote both humoral and cellular immune responses.

To overcome the abovementioned challenges in MERS-CoV vaccine development, the nanoparticle vaccine prepared herein integrates recombinant MERS-CoV RBD antigens with cyclic diguanylate monophosphate (cdGMP), a canonical STING agonist, known to promote Th1 immune responses and cellular immunity against the infectious threat. The RBD antigen-coated nanoparticles possess a virus-like morphology and can coordinately deliver both antigen and adjuvant in vitro and in vivo. In comparison to formulations that contain soluble antigens and adjuvants, inoculation with the nanoparticle (NP)-based vaccine induced greatly enhanced antigen-specific humoral and cellular responses in immunized mice. We further demonstrated that immunization with this NP-based MERS-CoV vaccine confers the protection against lethal MERS-CoV challenges in highly MERS-CoV-permissive transgenic mice globally expressing human dipeptidyl peptidase 4 (hDPP4), a functional MERS-CoV receptor. As the viromimetic nanoparticles are comprised entirely of biocompatible materials, this synthetic approach not only affords a safe and viable strategy in bridging the effectiveness between subunit and virus-based vaccines, but also provides a robust and versatile platform toward addressing the public health demand for vaccine development.

2. Results

2.1. Preparation and Characterization of STING Agonist-Loaded Hollow Polymeric Nanoparticles

The capsid-like hollow nanoparticles were prepared using a double emulsion process with 10 000 Da PLGA. Characterizations by cryo-EM and the dynamic light scattering (DLS) analysis revealed that the hollow nanoparticles had a shell thickness of ≈10 nm and a unimodal particle distribution with an average diameter of 114.0 nm (Figure 1B–D). A large aqueous interior could be observed, and successful encapsulation of cdGMP was verified by HPLC (Figure 1E). On the other hand, no peak of nanoparticle-associated cdGMP was detected after directly mixing hollow nanoparticles with cdGMP, indicating there is no interaction between the nanoparticle and the adjuvant (Figure S1, Supporting Information). With different cdGMP input, loading efficiency was consistent at approximately 48% (Figure 1F). This result indicates consistent partitioning of cdGMP solutions inside the hollow nanoparticles regardless of cdGMP concentration, thereby enabling controllable adjuvant loading for vaccine development. The cdGMP-loaded nanoparticles (NP(cdGMP)) are highly robust as little adjuvant release was observed over an extended period of time upon storage in enclosed Eppendorf tubes at 4 °C and room temperature (Figure S1, Supporting Information). In a dialysis experiment at 37 °C, (NP(cdGMP)) slowly released the adjuvant in a sustained manner at pH 7.4 but had a burst release profile at pH 5. This pH-sensitive release kinetics could be attributed to the acid-labile ester hydrolysis of PLGA under acidic conditions (Figure 1G). The release profile is favorable for vaccine delivery as the nanoparticles can retain their content upon administration and unload their cargoes once entering the acidic endolysosomal compartment following cellular uptake.

The structure of the hollow nanoparticles is reminiscent of self-assembled polymersomes[16] and single-emulsion-based

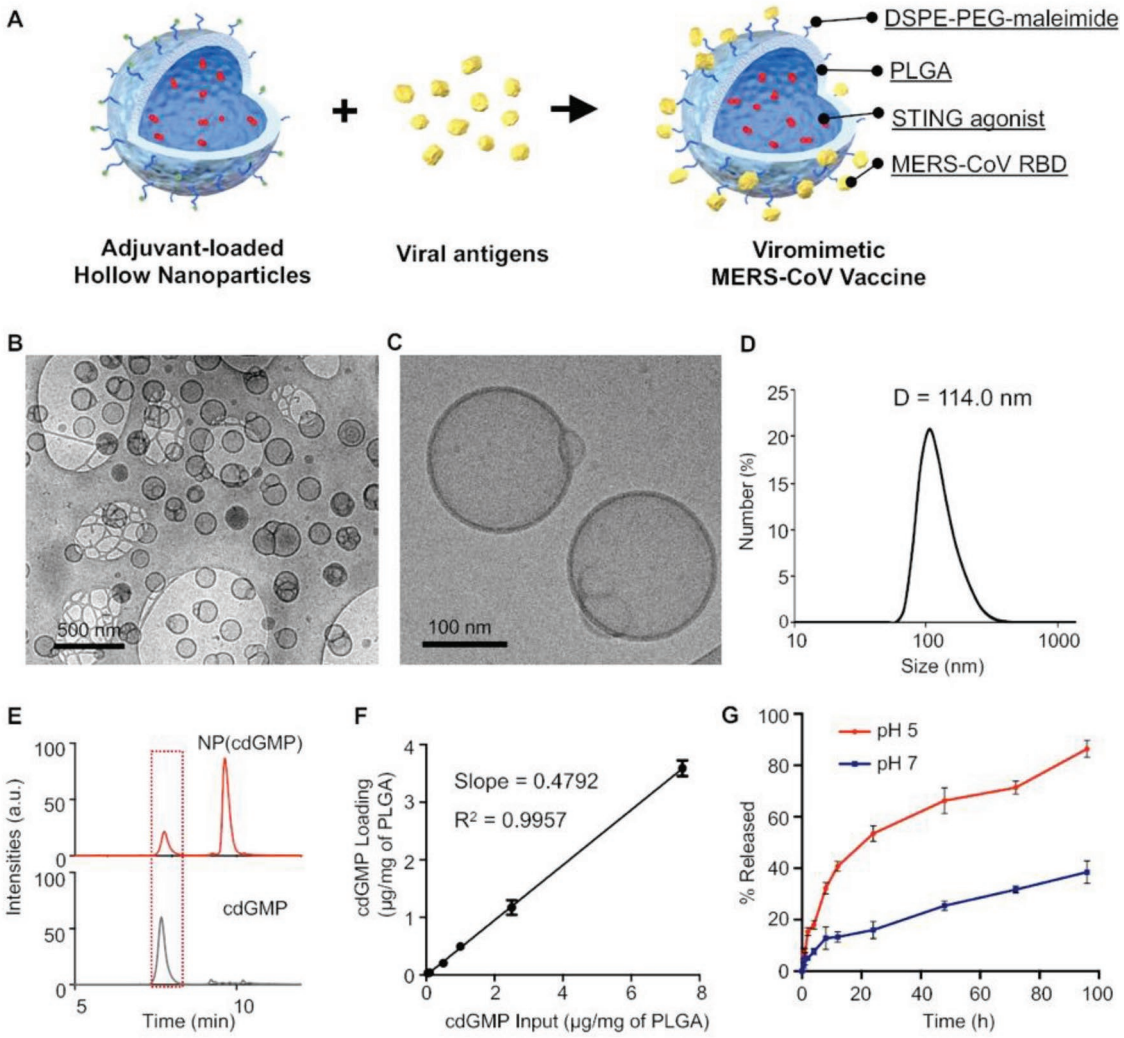

Figure 1. Characterization of adjuvant-loaded viromimetic nanoparticles. A) A schematic showing the preparation of viromimetic nanoparticle vaccine. Hollow PLGA nanoparticles with encapsulated adjuvant and surface maleimide linkers were prepared using a double emulsion technique. Recombinant viral antigens were then conjugated to the surface of nanoparticles via thiol-maleimide linkage. B,C) Cryo-electron microscopy of cdGMP-loaded hollow nanoparticle. D) Size distribution of nanoparticles determined by dynamic light scattering (DLS). E) HPLC diagram of adjuvant-loaded nanoparticles (NP(cdGMP)) and soluble cdGMP. F) cdGMP encapsulation efficiency at different adjuvant inputs. G) In vitro release profiles of cdGMP from PLGA hollow nanoparticles at pH 5 and pH 7. Error bars represent mean ± standard deviation ($N = 3$).

crystalsomes,[17] which possess sub-20 nm polymeric shells and large interior aqueous cores. Unlike these previously reported formulations, a double-emulsion process is adopted in the present work to facilitate the incorporation of water-soluble, nonionizable compounds. Upon adjusting the double emulsion parameters, we observed that the molecular weight of the polymer is critical to the hollow nanostructure formation. Preparations with 40 000 Da PLGA yielded solid particles or particles with miniscule aqueous interior as observed under cryoEM (Figure S1, Supporting Information), which are consistent with prior reports on double-emulsion-based PLGA nanoparticles.[18] These particles had poor cdGMP loading, which is also in agreement with previous, unsuccessful efforts on emulsion-based STING agonist encapsulation[9b] and reflect the long-standing challenge in nanoencapsulation of nonlipophilic compounds.[19] Successful preparation of the capsid-like hollow nanoparticles was made possible with the 10 000 Da polymer, which exhibits significantly lower viscosity in organic solvent as compared to the high-molecular-weight polymer (Figure S1, Supporting Information). Given the correlation between solution viscosity and surface tension,[20] it can be reasoned that double emulsions with the low-molecular-weight polymer solution had reduced interfacial surface tensions, thereby contributing to more stable core–shell structures and highly efficient incorporation of the cdGMP solution.

2.2. STING Agonist-Loaded Nanoparticles Enhance Localized Immune Potentiation and Reduce Systemic Reactions

For the subsequent studies, NP(cdGMP) containing 1.2 μg cdGMP mg^{-1} of PLGA was applied. The particular formulation

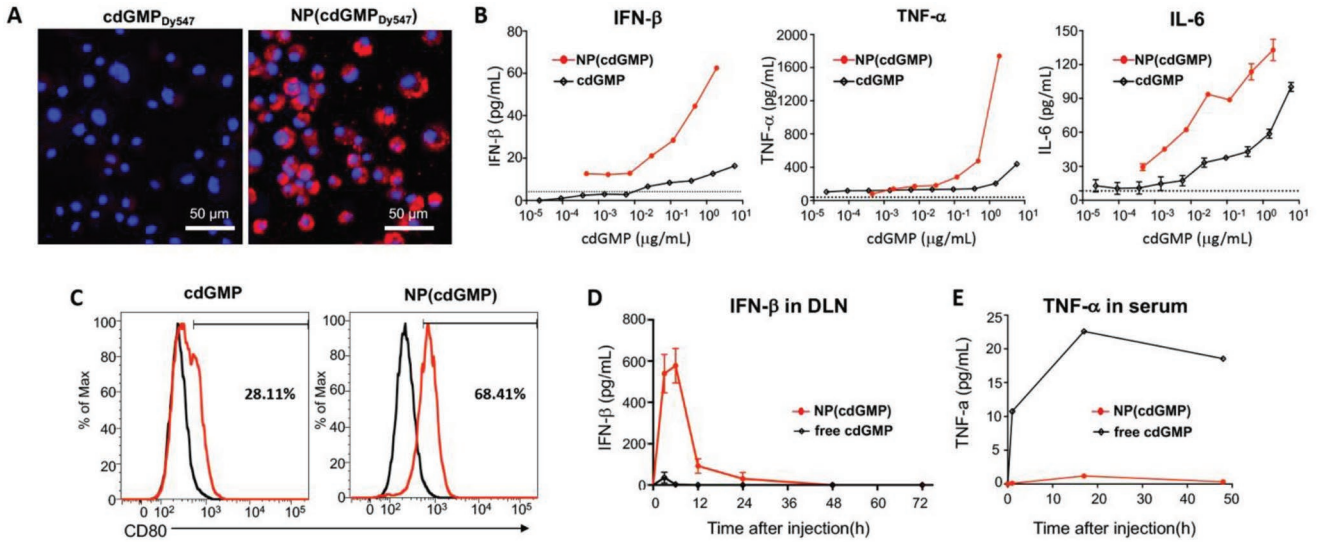

Figure 2. Nanoparticle encapsulation enhances the potency and reduces the reactogenicity of cdGMP. A) Cellular uptake of soluble and nanoparticle-encapsulated Dy-547-labelled cdGMP in JAWS II cells. B) Production of IFN-β, TNF-α and IL-6 by JAWS II cells treated with soluble cdGMP or cdGMP-loaded nanoparticles for 48 h. C) Upregulation of CD80 in bone marrow-derived dendritic cells incubated with 1 μg mL^{-1} of soluble or nanoparticle-encapsulated cdGMP for 24 h. Levels of D) IFN-β in the local draining lymph nodes and E) TNF-α in sera were analyzed by ELISA in C57BL/6 mice injected with soluble cdGMP or cdGMP loaded nanoparticles at the footpad. Error bars represent mean ± standard deviation ($N = 3$).

contained approximately 1000 cdGMP molecules per particle as calculated with particle numbers measured by nanoparticle tracking analysis (≈10^{12} particles per 1 mg of polymer). To assess the immune potentiating functionality of the nanoparticulate STING agonists, we first compared cdGMP and NP(cdGMP) in in vitro studies with murine dendritic cell (DC)-like JAWS II cells. JAWS II cells have been widely used in immunological studies due to their ease of preparation compared to primary dendritic cells.[21] Though slightly less responsive, JAWS II cells exhibit similar phenotypic markers and functions to bone marrow-derived dendritic cells (BMDCs).[22] Using a fluorescently labeled cdGMP, we noted that the cellular uptake of water soluble STING agonist was greatly increased when it was encapsulated in the hollow nanoparticles (**Figure 2**A), concomitant with an increase in the induction of cytokines, including IFN-β, TNF-α, and IL-6 (Figure 2B). The capability of cdGMP and NP(cdGMP) in inducing DC maturation was further confirmed by examining the upregulation of costimulatory molecules, such as CD80 and CD86, on BMDCs. At an equivalent adjuvant dosage (1 μg mL^{-1}), NP(cdGMP) significantly enhanced CD80 expression on BMDCs compared to free cdGMP (Figure 2C). These data indicate that the NP(cdGMP) is superior to free cdGMP in triggering host immune responses, in part, due to its more efficient uptake by professional antigen-presenting cells.

To further verify the advantage of NP(cdGMP) in promoting immune activation at the draining lymph node and in preventing undesirable or even harmful systemic proinflammatory responses, we measured the levels of IFN-β and TNF-α in the popliteal lymph nodes and sera derived from mice primed with NP(cdGMP) and free cdGMP. The mice treated with NP(cdGMP) had prominent levels of IFN-β within the draining lymph nodes (Figure 2D), yet TNF-α in the circulation was significantly subdued as compared to mice receiving free cdGMP (Figure 2E). The later observation likely indicated that the free cdGMP rapidly diffused into the blood stream upon administration, subsequently causing unfavorable systemic inflammatory responses. These data suggest that NP(cdGMP) can preferentially target the lymphatic system (i.e., draining lymph nodes), prompting localized immune activation while reducing systemic reactogenicity.

2.3. Construction of Synthetic MERS-CoV Nanoparticle Vaccine

To enable viral mimicry of synthetic nanoparticles as well as to provide the antigen source for vaccination, a recombinant RBD protein of the MERS-CoV spike antigen was produced using a baculoviral expression system (Figure S2, Supporting Information). After purification by FPLC, the identity of RBD protein was initially verified by its size at approximately 37 kDa with SDS-PAGE followed by the Western blot analysis with MERS-CoV-specific polyclonal antibody (Figure S2, Supporting Information). To facilitate RBD coupling with NP(cdGMP), the nanoparticles were prepared with DSPE-PEG-maleimide in the outer aqueous phase. Incorporation efficiency of the surface linkers was approximately 70%, yielding NP(cdGMP) with ≈3000 maleimide linkers per particle with negligible influence on cdGMP encapsulation efficiency (Figure S3, Supporting Information). A sulfhydryl-reactive cross-linker chemistry was adopted to conjugate the endogenous cysteine residues in RBD proteins to nanoparticle surfaces. Following the protein conjugation, the size of nanoparticles increased from 114.0 to 148.8 nm, and the zeta-potential shifted from −62.6 to −18.2 mV (**Figure 3**C). The polydispersity index (PDI) remained constant before and after protein conjugation, with a mean at 0.153 and 0.152, respectively (Figure S3, Supporting Information). Quantification by BCA assay showed that

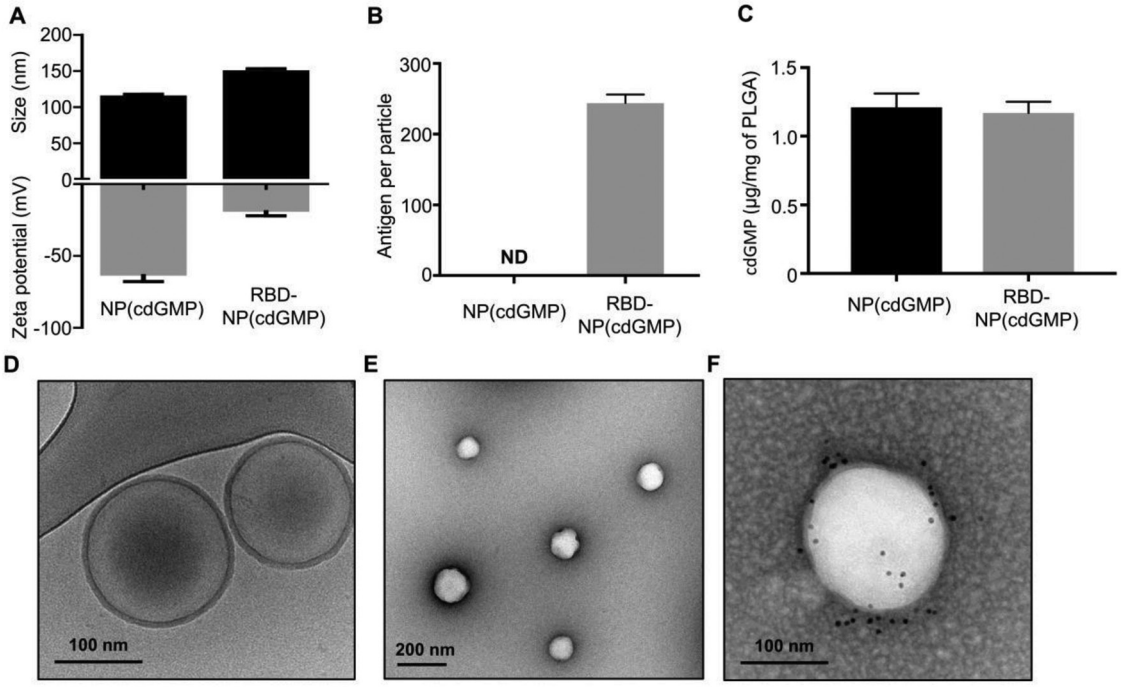

Figure 3. Physicochemical properties of the MERS-CoV nanoparticle vaccine. A) Size and zeta potential of adjuvant-loaded nanoparticles before and after the MERS-CoV RBD antigen conjugation. B) Estimated numbers of MERS-CoV RBD antigens on each PLGA hollow nanoparticle. Nanoparticle-attached antigens were calculated by directly quantifying protein contents on nanoparticles after conjugation reaction using the BCA protein assay. C) Loading of cdGMP in synthetic hollow nanoparticles before and after conjugation with recombinant MERS-CoV RBD antigens. D) Cryo-electron microscopy and E) transmission electron microscopy of MERS-CoV RBD coated nanoparticles. F) Immunogold staining of the MERS-CoV RBD conjugated nanoparticle with anti-His tag and goat antimouse IgG antibodies followed by transmission electron microscopy. Error bars represent mean ± SEM ($N = 3$).

RBD-conjugated nanoparticles (RBD-NP(cdGMP)) contained ≈70% of the antigen input, or ≈11.2 μg of RBD per mg of PLGA. With approximately 1×10^{12} particles per mg of PLGA, this corresponds to ≈250 protein antigens per particle (Figure 3D and Figure S3, Supporting Information). Cryo-EM images further revealed that the hollow particulate structure remained intact following protein conjugation (Figure 3E). It should be noted that the nanoparticles appeared solid in structure upon negative staining under TEM, in which uranyl acetate was precluded from entering the inner core, indicating the structural integrity of the polymeric shell (Figure 3F). Through immunogold staining, the presence of RBD antigens on the viromimetic nanoparticles was further confirmed (Figure 3G). We also observed that the protein conjugation process had little influence on the encapsulated adjuvant content (Figure 3H), which highlighted the particle's stability for surface functionalization.

2.4. Viromimetic Nanoparticles Enable Antigen and Adjuvant Codelivery In Vitro and In Vivo

Since coordinated delivery of antigens and danger signals is a fundamental attribute of viral vector-based vaccines and has been shown to improve subunit antigen immunogenicity,[4] we evaluated the antigen and adjuvant distribution by the viromimetic nanoparticles using AlexaFluor-488 labeled RBD antigens and Dy-547 labeled cdGMP. Following 24 h of incubation with JAWS II cells, prominent antigen and adjuvant fluorescence signals were observed intracellularly (**Figure 4**A). At a high magnification, colocalization of the antigen and adjuvant signals was evident, indicating the viromimetic nanostructure remained stable in the medium condition for cellular uptake. We further examined the distribution of RBD-NP(cdGMP) following subcutaneous administration in mice. One hour after the nanoparticle injection, colocalized antigen and adjuvant signals were observed in the draining lymph node. Further examination of $CD169^+$ cells, which are subcapsular sinus (SCS) macrophages responsible for capture and recognition of viruses and particulate antigens,[23] showed that a large number of the nanoparticles were colocalized with these "gatekeeping" cells (Figure 4B). This distribution of the nanoparticle is reminiscent of previous studies showing colocalization of virus virions and $CD169^+$ SCS macrophages in the draining lymph node following footpad injection.[24] The observation highlights the virus-like distribution of the nanoparticles, which synchronize lymph node delivery of surface-coated antigens and interiorly loaded adjuvant for better immune cell engagement and antigen presentation.

2.5. Viromimetic Nanoparticles Induce Heightened and Durable Humoral and Cellular Immune Responses

To determine the immunogenicity of the nanoparticle vaccine, groups of C57BL/6 mice were vaccinated subcutaneously with the RBD-NP(cdGMP), free RBD antigen admixed with free cdGMP, or free RBD antigen admixed with MF59 (Addavax),

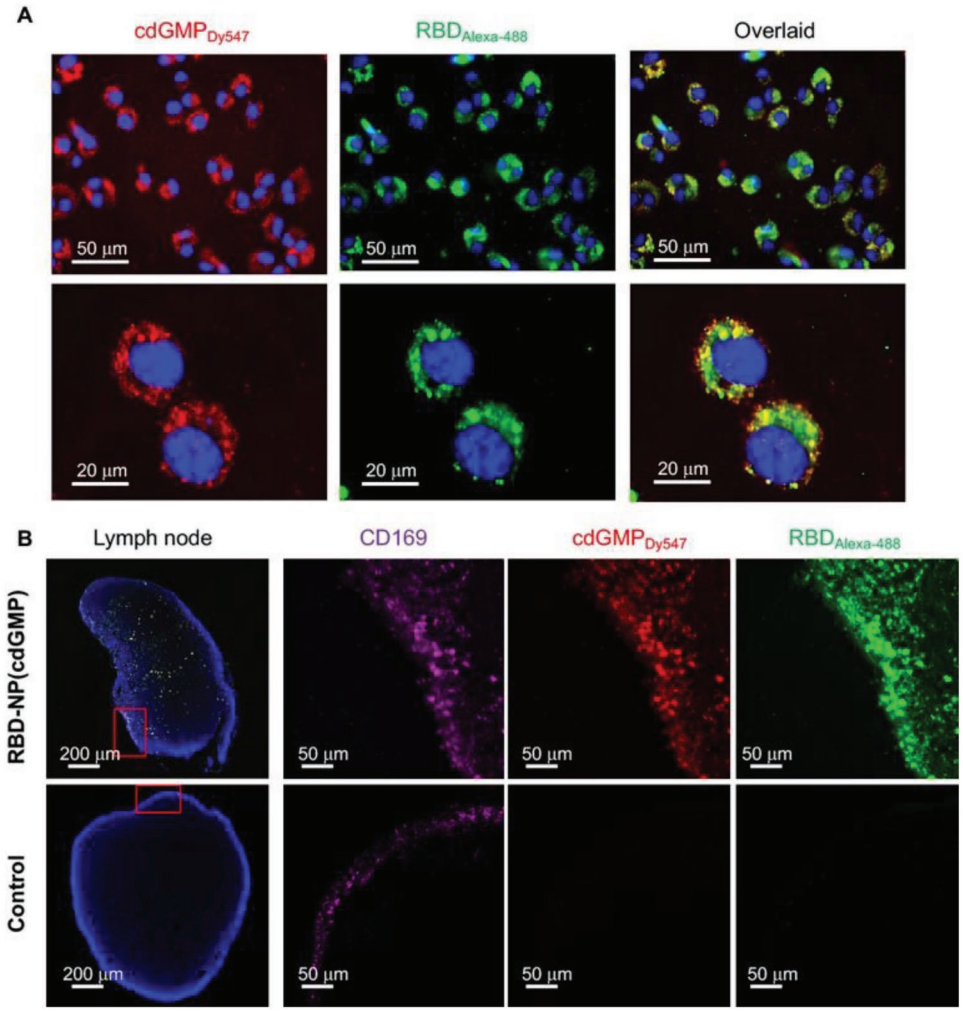

Figure 4. Synthetic viromimetic nanoparticles facilitate coordinated delivery of antigen and adjuvant in vitro and in vivo. A) Cellular distribution of Dy-547 labeled cdGMP (red) and AlexaFluor-488 labeled recombinant MERS-CoV RBD antigen (green) in JAWS II cells following 24 h of incubation with RBD-NP(cdGMP). B) Localization of AlexaFluor-488 labeled RBD antigen and Dy-547 labeled cdGMP in the draining lymph node of C57BL/6 mice subcutaneously injected with RBD-NP(cdGMP). Lymph nodes were collected at 3 h postinjection, and then processed followed by confocal microscopic analysis.

a clinically used adjuvant for influenza vaccines. Following a prime-boost vaccination on day 0 and day 21, sera were collected over a span of 300 d for ELISA analysis. Compared to other groups, RBD-NP(cdGMP) induced significantly higher titers of antigen-specific antibodies that reached a peak two weeks post-boosting and sustained for 300 d (**Figure 5**A). Notably, IgG subtype analysis on the sera collected on day 35 at the peak of the antibody response showed high levels of RBD-specific IgG2a antibodies in mice immunized with the nanoparticle vaccine, exhibiting a balanced Th1 and Th2 response (Figure 5B). In contrast, free MF59 and cdGMP-adjuvanted RBD antigens induced weak IgG1 responses and very limited levels of IgG2a. As Th1-associated responses and durable antibody titers are likely attributed to the help of $CD4^+$ T cell, we next investigated RBD-specific $CD4^+$ T cell responses elicited by different vaccine formulations. T cell responses at the acute phase were first determined seven days after the booster vaccination by restimulating harvested splenocytes with purified RBD antigens.[25] Following intracellular staining and flow cytometric analysis, RBD-NP(cdGMP)-inoculated group showed the highest frequency of IFNγ^+ subset that corresponds to functional, antigen-specific $CD4^+$ T cells (Figure 5C). Moreover, on week 6 postboosting after the transition of effector cells into stable memory populations,[25] $CD4^+$ T cells with the central memory phenotype ($CD44^+CD62L^+$) were also significantly elevated in the draining lymph nodes of RBD-NP(cdGMP)-immunized mice (Figure 5E). The antigen-specific $CD4^+$ T cell as well as the expanded central memory population elicited by the viromimetic nanoparticles can be thus associated with the augmented induction of anti-MERS-CoV RBD antibodies, particularly the Th1-associated IgG2a.

2.6. Viromimetic Nanoparticles Induce Antigen-Specific $CD8^+$ T cell Responses

We further evaluated $CD8^+$ T cell-mediated immunity, which has been shown to play a critical role in conferring protection against

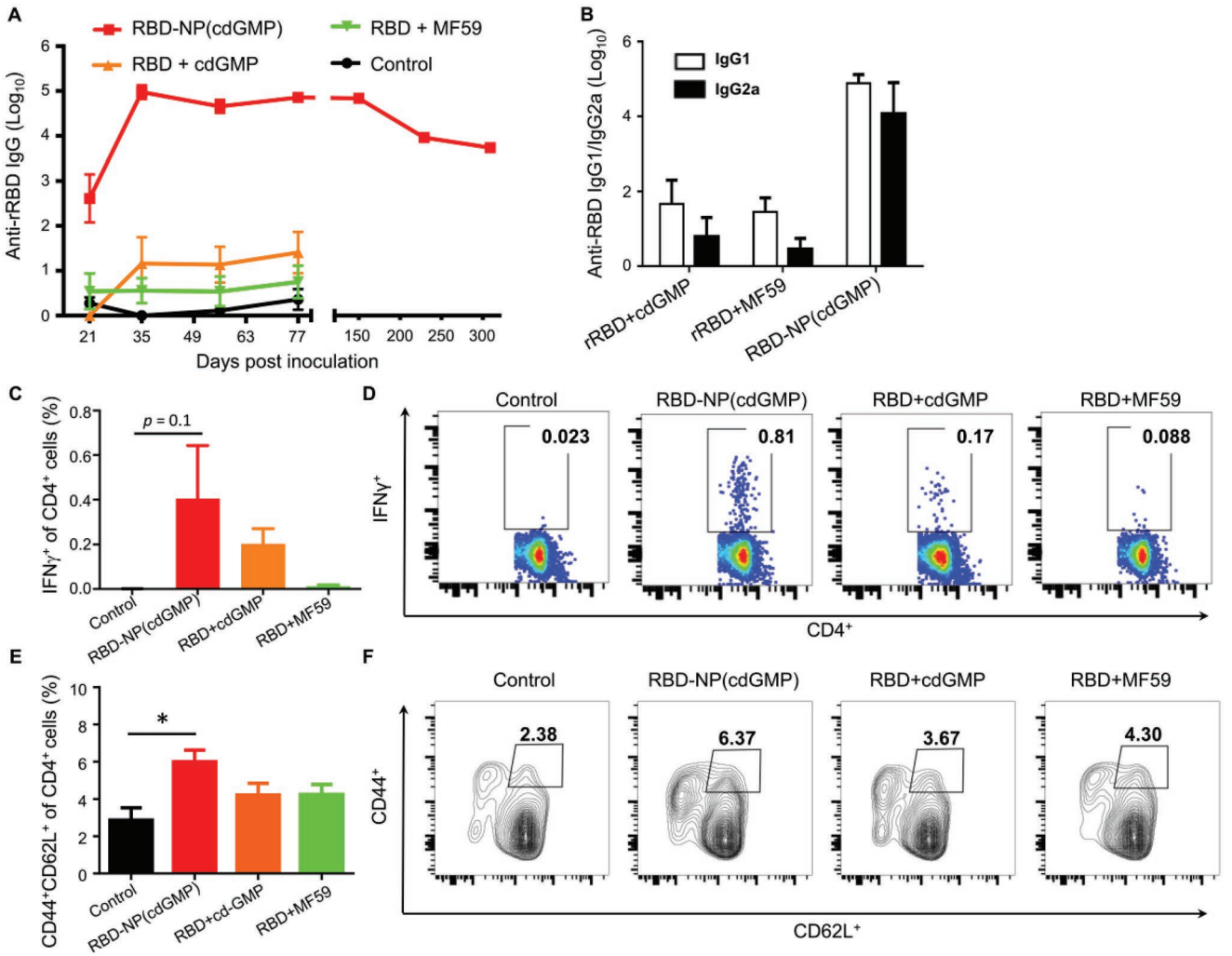

Figure 5. Robust and persistent humoral and CD4$^+$ T cell responses were induced in viromimetic nanoparticle-immunized mice. A) MERS-CoV RBD-specific antibody titers in C57BL/6 mice immunized with PBS, MERS-CoV RBD with soluble cdGMP or MF59, or RBD-NP(cdGMP) via the subcutaneous route. Error bars represent mean ± SEM ($N = 6$). B) MERS-CoV RBD-specific IgG1 and IgG2a titers in immunized mice on day 35 post-vaccination. Error bars represent mean ± SEM ($N = 6$). C,D) CD4$^+$ T cell responses against MERS-CoV RBD in immunized mice were determined by intracellular cytokine staining on day 7 after boost. Error bars represent mean ± SEM ($N = 3$). E,F) Frequencies of central memory (CD44$^+$CD62L$^+$) CD4$^+$ T cell in the draining lymph nodes of immunized mice 28 d after boosting. Error bars represent mean ± SEM ($N = 3$). Statistical analyses were performed by unpaired t tests ($^*p < 0.05$).

MERS-CoV infection.[15a,26] Several peptides, including S366, S395, S483, and S434, were identified and validated by our group and others as epitope targets for MHC class I antigen binding.[27] Following stimulating splenocytes with pooled peptides and intracellular IFN-γ–staining, only the nanoparticle-immunized mice showed a distinct population of IFN-γ-producing CD8$^+$ cells (**Figure 6**A), indicating the viromimetic nanoparticles were superior in inducing cytotoxic CD8$^+$ T cells than the control formulations. We further dissected the nanoparticle vaccine-induced CD8$^+$ T cell response using individual synthetic peptides, and we found that the majority of the RBD-specific CD8$^+$ T cell response elicited by the nanoparticle vaccine targeted S395, followed by S483, and S434 (Figure 6C). These data demonstrate that in addition to the robust antibody responses, the nanoparticle vaccine is able to prime the cellular arm of the immune system against the target recombinant RBD antigen.

2.7. Virus-Mimetic Nanoparticle Vaccine confers Protection against MERS-CoV Challenge in hDPP4 Transgenic Mice

We further evaluated the immunogenicity, protective efficacy, and safety of this nanoparticle vaccine against MERS-CoV infection in a proof-of-principle study by using highly permissive hDPP4 transgenic mice. Briefly, aliquots of RBD-NP(cdGMP) were stored at –20 °C and transported overseas for assessment in human DPP4-transgenic mice. Upon validating that the nanoparticles retained their expected size, surface antigens, and adjuvant encapsulants following a 2-month storage period (Figure S4, Supporting Information), both RBD-NP(cdGMP) and NP(cdGMP), which is without conjugated RBD, were administered subcutaneously to the transgenic mice on day 0 and day 28 (**Figure 7**A). Four weeks after the second immunization, sera were collected for determining

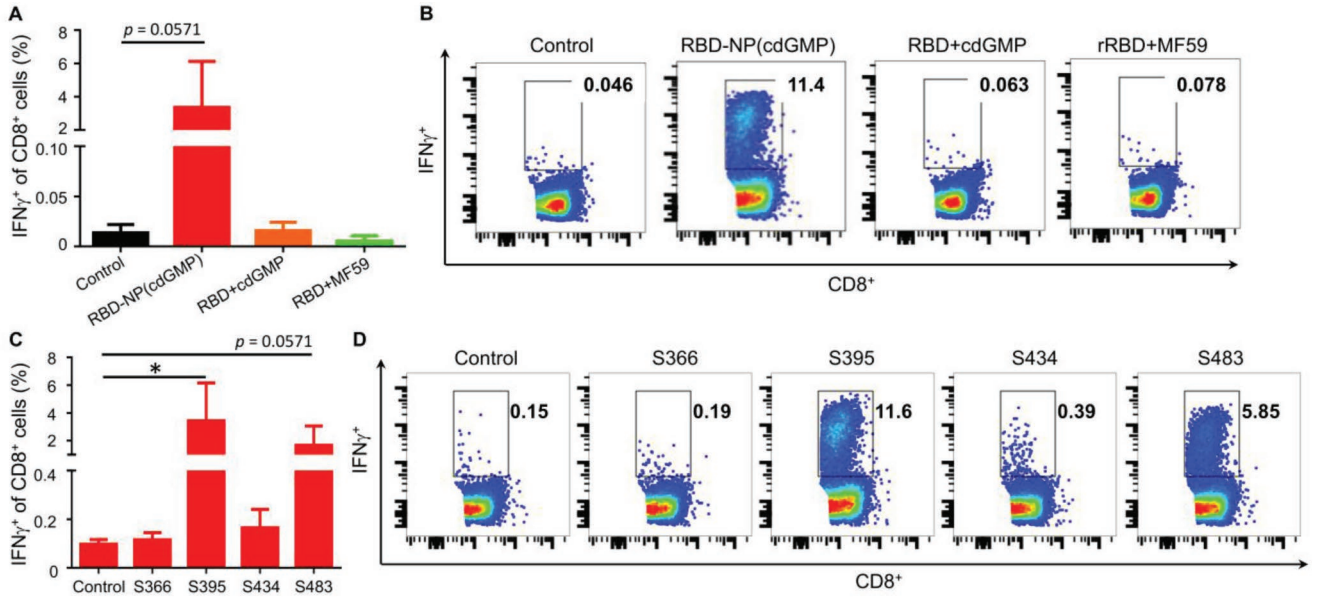

Figure 6. Viromimetic nanoparticle vaccine elicited strong $CD8^+$ T cell responses against MERS-CoV RBD. A,B) $CD8^+$ T cell responses against MERS-CoV RBD in the spleen of immunized mice were determined by intracellular cytokine staining on day 7 after boost. C,D) Peptide-specific $CD8^+$ T cell responses were assayed on day 7 after boost by restimulating splenocytes with MERS-CoV RBD-derived peptides followed by intracellular cytokine staining. Error bars represent mean ± SEM ($N = 4$). Statistical analyses were performed by unpaired t tests. (*$p < 0.05$).

the neutralizing antibody titers against live MERS-CoV using a Vero E6 cell-based microneutralization assay. Compared to the undetectable antibody response of the control NP-immunized animals, an average 100% neutralization titer (NT_{100}) of 128, ranging from 40 to 320 could be readily detected in each mouse immunized with RBD-NP(cdGMP) (Figure 7B and Table S1, Supporting Information). Following intranasal challenge with 100 LD_{50} (≈10^3 $TCID_{50}$) of MERS-CoV EMC/2012 strain, two mice from each group were euthanized at 2 d postinfection (dpi) for assessing the viral loads and the histopathology of the lungs, whereas the remaining mice were monitored daily for the mortality until 24 dpi. As safety concerns of vaccination-induced immunopathology have been raised in MERS-CoV and SARS-CoV infection models with whole inactivated virus (WIV), recombinant DNA-based, and even modified vaccinia virus Ankara (MVA) vectored vaccines,[28] we thoroughly examined the pathological changes of lung specimens of challenged mice. Although no any eosinophilic infiltration could be readily observed in either group (Figure 7C and Figure S5, Supporting Information), mice immunized with RBD-NP(cdGMP) exhibited a mild infiltration of lymphocytes and monocytes as compared to the control nanoparticles (Figure 7C and Figure S5 in the Supporting Information, blue arrows). While the exact nature of eosinophil-free inflammatory responses warrants further investigations, we speculate that the enhanced Th1 responses afforded by the nanoparticle vaccine might be accountable.[29] Given the potent antigen-specific T-cell responses induced by the RBD-NP(cdGMP) and the high viral titer used for the animal challenge, it is likely that the lymphocytic infiltration corresponded to local recruitment of vaccine-induced lymphocytes. The presence of such local lymphocytes has been reported to contribute to protective immunity against the respiratory virus.[30]

The viral titers in the animals sacrificed at 2 dpi were subsequently assessed. No infectious progeny virus was recovered from mice immunized with RBD-NP(cdGMP), compared to moderate, but readily detectable yields of infectious virus in control NP-immunized mice (Figure 7D). Quantification of the viral loads by quantitative RT-PCR analyses also showed a significant reduction in the amount of MERS-CoV RNA in RBD-NP(cdGMP)-immunized mice (Figure 7E), demonstrating effective containment of viral spread and replication. Furthermore, mice immunized with RBD-NP(cdGMP) uniformly survived at 24 dpi upon termination of the study. In contrast, all of the control NP-immunized mice succumbed to infection within 16 dpi ($p = 0.0246$) (Figure 7F). These results of the pilot study validate the efficacy and safety of the NP-based MERS-CoV RBD/cdGMP vaccine against MERS-CoV infection and disease. Additional studies are warranted to comprehensively develop this vaccine candidate against the emerging infectious threat.

3. Discussion

Prioritized by WHO for vaccine research, MERS-CoV is a prominent example of emerging pathogens with an urgent public health need for preventative measures. Sporadic outbreaks of the disease continue to be reported with a high mortality rate at ≈35%, and there are no clinically approved vaccines against the pathogen to this date. While candidates include a DNA-based candidate,[31] an adenovirus-based candidate,[12a] and an MVA-based vaccines[32] have entered clinical trials, much ongoing research efforts on MERS-CoV vaccination are focused on recombinant protein subunit vaccines owing to their safety and production consistency. In the present study, MERS-CoV antigens are formulated with synthetic nanoparticles in a virus-like fashion to improve

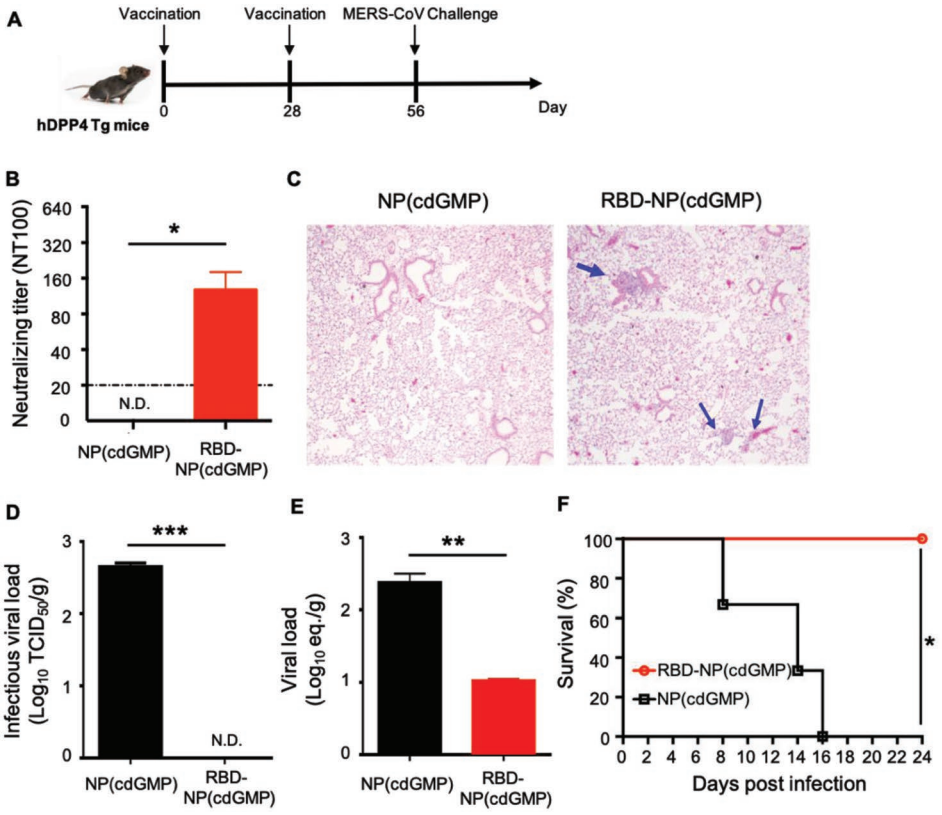

Figure 7. Viromimetic nanoparticle vaccine confers protection against MERS-CoV infection in DPP4 transgenic mice. A) A schematic diagram of the vaccination and MERS-CoV challenge schedule in human DPP4-transgenic mice. B) Titers of 100% neutralizing serum antibody (NT_{100}) against MERS-CoV in immunized mice. Dashed line represents a limit of detection at 1 in 20 dilution. Error bars represent mean ± SEM ($N = 5$). C) Representative graphs of hematoxylin-eosin staining of lung sections in immunized mice on day 2 postchallenge. Arrows indicate lymphocyte infiltration. Determination of infectious viral loads in the lung of immunized mice on day 2 after MERS-CoV challenge using D) a Vero E6 cell-based assay and E) quantitative PCR. Error bars represent mean ± SEM ($N = 2$). Statistical analyses were performed by unpaired t tests ($^*p < 0.05$, $^{**}p < 0.01$, $^{***}p < 0.001$). F) Survival of MERS-CoV challenged mice ($N = 3$) ($^*p < 0.05$).

vaccine potency. Among the commonly used MERS-CoV antigens, namely full-length S protein, S1 fragment, and RBD, RBD is herein selected as antibodies against this domain have shown greater virus neutralizing potential compared to the other candidates.[33] Prior studies have adopted S protein-based nanoparticles and RBD-human Fc conjugates to enhance the immunogenicity of MERS-CoV antigens.[34] As MERS-CoV RBD protein by itself is poorly immunogenic[50], the present nanoparticle vaccine integrates the antigen with cdGMP to promote antibody and T cell responses, thereby obviating the need for human Fc conjugation.

Lessons learnt from SARS-CoV vaccine development as well as prior MERS-CoV vaccine studies indicated that immunologic adjuvants, particularly Th1-biased adjuvants, are critical for improving antigen immunogenicity and reducing eosinophilic immunopathology. However, administration of these adjuvanted formulations needs to be handled with caution as the elevated levels of immunogenicity usually come at the cost of increased systemic inflammatory responses and reactogenicity. The safety concern regarding adjuvant reactogenicity has motivated ongoing development of particulate adjuvant formulations,[35] which have been designed to target the lymphatic system to better promote localized immune responses. For the CDN-based, STING agonist adjuvant adopted in the present study, several vehicles, including liposomes,[9a,36] calcium phosphate nanoparticles,[37] polymeric microparticles,[38] and cationic polymers,[39] have been applied to improve the molecule's potency and safety in prior reports. Compared to the aforementioned STING agonist formulations, the hollow polymeric nanoparticle developed herein possesses the combined advantages of biocompatibility, size consistency, colloidal stability, tunable adjuvant loading, pH-responsive release, and antigen functionalizability. These favorable attributes make the hollow nanoparticles a desirable delivery platform for STING-mediated immune modulation. Examination of the NP(cdGMP) showed many of the reported advantages of nanoparticulate adjuvants, including efficient uptake by antigen presenting cells, enhanced immunostimulating capability, and reduced systemic inflammatory responses. These attributes are expected to improve the immunogenicity, efficacy, safety, and applicability of STING agonists for MERS-CoV and other vaccination purposes. In addition, recombinant viral antigens can be attached to these adjuvant-loaded nanoparticles, enabling mimicry of natural virions for effective immune potentiation and induction of protective immune responses.[40]

The co-presence of danger signals during antigen processing by dendritic cells has been identified as an important factor in

self/nonself discrimination,[4] and codelivery of antigen and adjuvants by a single carrier has been shown to enhance immune cell activation and antigen presentation. The timing between type I IFN signaling and antigen presentation has also been observed to critically influence immune responses; whereas IFN signaling following antigen presentation (in-sequence signaling) potently stimulates T cell expansion, pre-exposure of T cells to IFNs prior to antigen presentation (out-of-sequence signaling) induces an inhibitory effect.[8] These findings highlight the significance of coordinated antigen and adjuvant delivery and support the viromimetic vaccine design on a mechanistic basis. Further to this point, literature has shown that excessive production of type I IFNs during infection can have detrimental effects on immune responses,[41] and adaptive immunity can be strongly influenced by the timing and magnitude of type I IFN administration[42] and STING activation.[43] While there are lingering concerns with the use of STING agonists as vaccine adjuvants given the pleiotropic role of type I IFNs, it is generally accepted that a short, strong type I IFN response in coordination with antigen presentation is conducive to adaptive immunity.[44] In light of this, the hollow nanoparticle offers an ideal controllable system that can precisely gauge the dosing and timing of type I IFN signaling for robust immune responses. Further study is warranted to systemically evaluate the concentrations of antigen and adjuvant for their influences on immune activation.

In the present work, we showed that in contrast to soluble RBD antigens formulated with free STING agonists or MF59, a robust and sustained MERS-CoV RBD-specific antibody response was observed in mice immunized with the virus-like nanoparticle vaccine. The data indicate that this viromimetic nanoparticulate vaccine was superior in its ability to mount humoral responses when compared to MF59, the state-of-the-art adjuvant for influenza vaccine. The antibody generated by the vaccine is capable of neutralizing to MERS-CoV and directly contributes to the protective immunity against viral challenges. Moreover, the nanoparticle vaccine induced a balanced Th1/Th2 immune response, which is consistent with prior reports of STING-agonist-mediated immune stimulation.[5a,6a,45] The potent Th1 response as indicated by the high levels of IgG2a antibodies likely accounted for the absence of eosinophilic immunopathology. Notably, our nanoparticle vaccines are highly capable of priming both antigen-specific $CD4^+$ and $CD8^+$ T cell responses. While there is a yet-to-be-consensus thought that the recovery of MERS-CoV infection may not solely correlate with antibody responses, recent literature is showing increasing emphasis on the role of T cell responses, especially $CD8^+$ T cells, in protective immunity against MERS-CoV.[15] Future studies further dissecting humoral and cellular immune responses in MERS-CoV protection are warranted.

Several vaccine candidates against human respiratory coronavirus, including whole inactivated virus (WIV), recombinant S, S1, or RBD subunit proteins, vectored- or DNA-based S or S1, and others, have been investigated in permissive mice, rabbits, and nonhuman primates (NHPs) against SARS-CoV and MERS-CoV infection.[46] While most of these vaccine candidates are immunogenic and effective in immunized animals against subsequent live virus challenges, concerns over their safety with regard to the induction of immunization-induced immunopathology and/or antibody-mediated disease enhancement (ADE) in immunized and challenged animals exist. These undesirable host responses are characterized by enhanced pulmonary eosinophilic and monocytic infiltration, accompanied by an increased recruitment of complement protein C3a without any sign of uncontrollable viral infection.[46] It was noted that passive transfer of sera that contain MERS-CoV-specific but non-neutralizing antibodies derived from infected or a full-length S protein-immunized rabbits to naïve rabbits resulted in exacerbated pulmonary inflammation, further accentuating the safety concern over suboptimal host responses to infection and/or immunization.[47] It has also been observed that live MERS-CoV challenge of highly permissive human DPP4 transgenic mice immunized with either alum- or MF59-formulated WIV uniformly caused significant increases in Th2-skewed eosinophilic infiltration within the lungs.[14] Recently, we noted human DPP4 transgenic mice immunized with recombinant adenovirus Ad5-encoding S1 (rASd5-S1) exhibited varying extents of perivascular hemorrhage within the lungs upon challenge despite its impressive immunogenicity and efficacy against the lethality of MERS-CoV.[48] In this study, the prototype nanoparticle-based MERS vaccine is not only immunogenic and effective in inhibiting viral infection, but also obviates the induction of undesirable lung pathology in immunized and challenged human DPP4 transgenic mice. These encouraging results warrant further development of the nanoparticle-based vaccine platform.

With MERS-CoV as a model pathogen, this study also demonstrates a viromimetic nanoparticle vaccine design that may be applicable to the many viral diseases threatening the public health. While live microbes have long provided design inspirations for vaccine engineering,[49] the present work further advances the pathogen-mimicking concept with the STING agonist-loaded, capsid-like hollow nanoparticles. Unlike most prior reports of PLGA-based nanoformulations that have inadequate encapsulation capacity for water-soluble compounds, the hollow PLGA nanoparticles presently herein permit tunable encapsulation and controlled release of water-soluble STING agonists. The cargo of the nanoparticles may be further adjusted to modulate immune stimulation, and the particles' functionalizability allows for attachment of different recombinant viral antigens to tailor to specific vaccination needs. Consisting entirely of biocompatible materials, the nanoparticles are safe to administer, and they can be stored and transported upon freezing. Although the need for cold chain transportation would incur additional cost, we anticipate the public health benefit to outweigh the technological and logistical investment. Toward future translation, scalable manufacturing is expected to benefit from existing infrastructures for recombinant protein production and polymeric nanoformulations.[50] By effectively coupling viral antigens with immunologic adjuvants, nanoparticle vaccines with minimal safety concerns and potency rivaling viral vector-based formulations can be envisioned.

4. Conclusions

Effective prophylactic measures against highly lethal pathogens have stringent safety and efficacy requirements, yet a safety/efficacy tradeoff often exists among commonly adopted viral-vector-based and subunit-protein-based vaccine candidates.

Using synthetic biodegradable polymers, we have constructed a virus-like hollow nanoparticle and associated it with a subunit antigen and an adjuvant. Through this nanoengineering approach, we demonstrated the preparation of a safe and potent vaccine formulation against Middle East respiratory syndrome coronavirus (MERS-CoV), which is a WHO-prioritized pathogen with an urgent vaccination need. The study highlights the application of synthetic nanoparticles for advancing vaccine technology against emerging infectious threats.

5. Experimental Section

Animals: C57BL/6 mice (National Laboratory Animal Center, Taiwan) were housed in the animal facility maintained by the Institute of Biomedical Sciences, Academia Sinica. Female transgenic mice expressing human DPP4 were generated and housed in the barrier facility at the University of Texas Medical Branch as previously described.[51] All experiments were performed under an approved protocol by the Institutional Animal Care and Use Committee (IACUC), Academia Sinica, or by the Office of Research Project Protections, IACUC, University of Texas Medical Branch, Texas.

Cell Lines: *Spodoptera frugiperda* Sf9 and serum-free adapted Sf21 cells were purchased from Invitrogen. Sf9 cells were cultured in Grace's medium (Thermo Fisher Scientific) supplemented with 10% fetal bovine serum (FBS), 100 U mL^{-1} penicillin, and 100 µg mL^{-1} streptomycin. Sf21 cells were cultured in Sf-900 II Serum free medium (Thermo Fisher Scientific) containing 100 U mL^{-1} penicillin, and 100 µg mL^{-1} streptomycin at 27 °C. Murine immature dendritic JAWS II cells were obtained from American Type Culture Collection, and maintained in minimum essential medium (MEM) alpha medium containing ribonucleosides, deoxyribonucleosides, 10% FBS, 4×10^{-3} M L-glutamine, 100 U mL^{-1} penicillin and 100 µg mL^{-1} streptomycin, 0.5×10^{-3} M 2-mercaptoethanol, 1×10^{-3} M sodium pyruvate, and 5 ng mL^{-1} murine GM-CSF in a humidified 37 °C incubator with 5% CO_2.

Recombinant MERS-RBD Expression and Purification: DNA sequence encoding the receptor binding domain (RBD) of the MERS-CoV spike antigen and a C-terminal 6 × histidine tag for affinity purification was obtained by DNA synthesis (Genscript), and then cloned into the pFastBac1-gp67-His-IRES GFP vector. The resultant recombinant plasmid was first amplified in *E. coli* DH5α, and transformed into *E. coli* DH10Bac for gene transposition. The transposed bacmid was then purified for transfection and preparation of baculoviruses carrying the recombinant MERS-CoV RBD in Sf9 cells. All the transformants were screened by colony PCR with appropriate primers, and the recombinant plasmid was verified by sequencing.

Baculovirus expression system was adopted for the production of the recombinant MERS-CoV RBD. Briefly, Sf21 cells were infected with the recombinant baculovirus at an MOI of 1 and incubated at 27 °C. Four days later, the culture supernatant was collected by centrifugation, and the extracellular RBD proteins were purified by the HisTrap HP column (GE Healthcare) using an FPLC system. The purified protein was verified by Western blot with mouse anti-His tag antibody (Roche) or antirecombinant MERS-CoV RBD rabbit serum. The protein concentration was determined by the Bradford assay (Bio-Rad).

Nanoparticle Vaccine Preparation: Hollow polymeric nanoparticles were prepared using a water-in-oil-in-water double emulsion process. A polymer solution was prepared by dissolving 50 mg mL^{-1} of carboxy terminated, 50:50 poly(DL-lactide-*co*-glycolide) (0.15–0.25 or 0.55–0.75 dL g^{-1}, corresponding to ≈10 000 and ≈40 000 Da, respectively; LACTEL Absorbable Polymers) in dichloromethane. Viscosity of the polymer solutions was quantified using a microVISC rheometer (RheoSense) according to the manufacturer's protocol. The inner aqueous phase was prepared by dissolving cdGMP (Invivogen) in 100×10^{-3} M of phosphate buffer (pH 7). For a typical preparation, 50 µL of aqueous solution containing 125 µg of cdGMP was emulsified in 500 µL of polymer solution in ice using an Ultrasonic Probe Sonicator under the pulse mode with 40% amplitude and on-off durations of 1 and 2 s for 1 min. The first emulsion was subsequently added to 5 mL of 1×10^{-3} M phosphate buffer (pH 7), which was then probe sonicated at 30% amplitude with on-off durations of 1 and 2 s for 2 min. The emulsion was subsequently poured to 8 mL of water and heated at 40 °C under gentle stirring in a fume hood for solvent evaporation. For preparing DSPE-PEG-maleimide-functionalized hollow nanoparticles for antigen conjugation, 900 µg of DSPE-PEG(2000)-maleimide (Avanti Polar Lipids, Inc.) was added to the 8 mL of water prior to the addition of second emulsion. Following 1 h of solvent evaporation, the nanoparticles were collected using 100 kDa MWCO Amicon filters (Sigma-Aldrich).

For conjugating recombinant MERS-CoV RBD antigens to the nanoparticles, purified RBD proteins were mixed with maleimide-functionalized nanoparticles in solutions containing a mild reducing agent (tris(2-carboxyethyl)phosphine; TCEP). For a typical vaccine preparation, 800 µg of RBD antigens were mixed with 50 mg of hollow nanoparticles containing ≈58 µg of cdGMP in 2 mL of solution comprised of 1×10^{-3} M of phosphate buffer (pH 7) and 1×10^{-3} M of TCEP. The mixture was incubated for 4 h under gentle shaking at room temperature, and the RBD-conjugated nanoparticles were isolated from free proteins using 100 kDa MWCO Amicon filters. Nanoparticle vaccines were stored by freezing in 10% sucrose.

Nanoparticle Vaccine Characterization: Nanoparticle concentration was evaluated by nanoparticle tracking analysis using NanoSight NS500 (Malvern Instrument) and nanoparticle size and zeta potential were determined by dynamic light scattering (DLS) using Zetasizer Nano ZS (Malvern Instrument). Adjuvant retention study was performed by suspending cdGMP-loaded nanoparticles in PBS at 10 mg mL^{-1} in Eppendorf tubes. At predetermined time points, nanoparticles were washed with an Amicon filter to remove released cdGMP and quantified for cdGMP content. cdGMP release kinetics in physiologically relevant conditions were characterized with a dialysis experiment in two different pH environments (pH 5 or 7), in which cdGMP-loaded nanoparticles were loaded in Slide-A-Lyzer MINI dialysis devices (10 kDa MWCO; Thermo Fisher Scientific) and collected at predetermined time points for cdGMP quantification.

Association of DSPE-PEG-Maleimide to the nanoparticles was analyzed by quantifying the nanoparticle-bound PEG using an iodine precipitation assay. Nanoparticle-conjugated recombinant MERS-CoV RBD protein was measured using the BCA protein assay (Thermo Fisher Scientific) following the manufacturer's protocol. For nanoparticle visualization, negative staining was performed with uranyl acetate and immunogold staining was performed using mouse anti-His tag antibody (Roche) and goat antimouse IgG (H+L) antibody conjugated with 6 nm colloidal gold (Jackson ImmunoResearch, West Grove, PA). Negatively stained and immunogold stained samples were visualized using an FEI 120 kV Sphera microscope, and Cryo-EM images were acquired using a Tecnai F20 transmission electron microscope (FEI Company, Netherlands) operating at an acceleration voltage of 200 kV.

Quantification of cdGMP Loading by HPLC Analysis: The loading of cdGMP in the hollow nanoparticle was quantified by high-performance liquid chromatography (HPLC) using an Ascentis Express C18 column (Sigma-Aldrich).[52] Briefly, hollow nanoparticles were lyophilized and then 95% acetone was added to disrupt the PLGA nanoparticle. After removing acetone on a 60 °C dry bath, samples were resuspended in 100 µL H_2O followed by analysis on an Agilent 1100 Series HPLC system. Samples containing cdGMP retrieved from acetone-treated nanoparticles and a set of cdGMP standards were analyzed using a gradient HPLC method in which the starting mobile phase consisted of a 97:3 mixture of 10×10^{-3} M ammonium acetate (AA) and acetonitrile (CAN). The second mobile phase was a 92:8 mixture of AA and CAN with a gradient time of 2 min, and the third mobile was set with a 97:3 mixture of AA and CAN with a gradient time of 8 min. Standard calibration curves for quantification of cdGMP were acquired ranging from 250 to 1.95 µg mL^{-1} with R^2 values close to 1.

Generation of Bone Marrow-derived Dendritic Cells (BMDCs): Bone marrow-derived dendritic cells were obtained from C57/BL6 mice

according to the protocol of Matheu et al. with minor alternations.[53] Briefly, bone marrow cells were harvested from femur bones, and cultured in Dulbecco's modified Eagle medium (DMEM) containing 10% FBS, 50×10^{-6} M β-mercaptoethanol, 20 ng mL^{-1} GM-CSF, and 10 ng mL^{-1} IL-4. The culture medium was replaced on day 3, and the cells were collected for experiments on day 7. Following flow cytometric analysis, >85% of the harvested cells showed characteristics of CD11c$^+$ BMDCs.

Immune Potentiation by cdGMP-Loaded Nanoparticles In Vitro and In Vivo: Dy-547-labelled cdGMP (BIOLOG LifeScience Institute) were used in the cellular uptake study. Free cdGMP or nanoparticle-encapsulated cdGMP were added to JAWS II cells. After 24 h of incubation, fluorescence images were acquired with IX-83 (Olympus). For in vitro immune activation, JAWS II cells were plated at a density of 1.6×10^5 cells per well in a 12-well plate. After 24 h, various concentrations of free cdGMP or nanoparticle-encapsulated cdGMP were added to the cells. Culture supernatants were harvested at 24 h (for IL-6) or 48 h (for TNF-α and IFN-β) following incubation for cytokine analysis using TNF-α mouse uncoated ELISA kit (Thermo Fisher Scientific), IL-6 mouse uncoated ELISA kit (Thermo Fisher Scientific), and mouse IFN-β ELISA kit (R&D systems) according to the manufacturers' instructions. For activation marker analysis, bone marrow-derived dendritic cells were incubated with FcR blocker on ice for 30 min, followed by 1:100 antimouse-CD80-FITC or IgG isotype control (eBioscience) incubation on ice for another 30 min in the dark. After incubation, cells were further washed three times and resuspended in 0.2 mL of PBS before flow cytometric analysis using FACS LSR II (BD Biosciences). Analysis was done by FlowJo software (Tree Star, Ashland, OR). For in vivo immune potentiation analysis, free cdGMP or nanoparticle-encapsulated cdGMP were inoculated to C57BL/6 mice via footpad injection. At various time points, mice sera were collected, and popliteal lymph nodes were homogenized in DMEM. Cytokines were measured by TNF-α mouse uncoated ELISA kit (Thermo Fisher scientific) and mouse IFN-β ELISA kit (R&D systems) from the serum and homogenate.

Imaging of Antigen and Adjuvant Delivery by Nanoparticles: JAWS II cells were incubated with nanoparticles containing Dy-547 labeled cdGMP and AlexaFluor-488 labeled RBD antigen for 24 h in 37 °C incubator. After removing the media, the cells were washed three times with PBS, and fixed with 4% paraformaldehyde followed by imaging on an Olympus IX-83 fluorescence microscope. For in vivo distribution, a modified method was adopted from the report by Gonzalez et al.[24a] Briefly, C57BL/6 mice were injected subcutaneously with the abovementioned Dy-547 cdGMP and AlexaFluor-488 RBD labeled nanoparticle. After 2.5 h, each mouse was injected with 1 µg of APC antimouse CD169 antibody (clone 3D6.112; BioLegend) via the same subcutaneous route and the draining lymph nodes were harvested after 30 min. The draining lymph nodes were cryo-sectioned and fixed with 4% paraformaldehyde followed by imaging using Zeiss LSM 700 confocal microscopy.

Animal Immunization and Serum Collection: Groups of C57BL/6 mice were immunized twice on day 0 and 21 subcutaneously at the tail base with one of the following formulations: MERS-CoV RBD nanoparticles, free RBD proteins mixed with free cdGMP or MF59 adjuvants (Invivogen), and PBS. Each mouse was given a 100 µL inoculum of 10 mg mL^{-1} nanoparticle containing 10 µg of recombinant RBD proteins and 1 µg of cdGMP, 10 µg of free RBD with 1 µg of free cdGMP, or 10 µg of free RBD with 50 µL of MF59. At designated time points, blood was collected from the facial vein into BD SST microtainers (BD Biosciences). Sera were obtained after centrifugation at 3000 × g for 10 min and stored at −20 °C.

ELISA Analysis: Flat-bottom microplates (Nunc, Denmark) were coated overnight with purified recombinant MERS-CoV RBD proteins (100 ng per well) at room temperature. After blocking with 5% (w/v) skim milk (BD Difco, Sparks, MD) at room temperature for 1 h, 100 µL of serially diluted mouse sera were added to each well, and incubated at room temperature for 1 h. Following three washes, 100 µL of 1:2000 diluted peroxidase-conjugated goat antimouse IgG (H+L), IgG1, or IgG2a (Jackson ImmunoResearch) was added into each well and incubated at room temperature for 1 h. Enzymatic reaction was carried out using 100 µL of SureBlue Reserve TMB Microwell Peroxidase Substrate (KPL, Gaithersburg, MD) and stopped by the addition of 100 µL of TMB stop solution (KPL). The optical density at 450 nm (OD_{450}) was measured using an automated plate reader (Thermo Fisher Scientific).

Intracellular Cytokine Staining and Flow Cytometric Analysis: Spleens or lymph nodes were collected from euthanized mice for analysis of CD4$^+$ or CD8$^+$ T cell responses by intracellular cytokine staining (ICS). Single cells were prepared from spleens or lymph nodes and plated at 1×10^6 cells per well into round-bottom 96-well plates. RBD antigens and synthetic peptides (S366 (S366–374; FEAKPSGSV), S395 (S395–402; QVYNFKRL), S483 (S483–491; TVPHNLTTI), and S434 (S434–441; ASNCYSSL)) were added at 37 °C with 5% CO_2 to stimulate CD4$^+$ and CD8$^+$ T cells respectively. After 4 h, GolgiPlug protein transport inhibitor (BD Biosciences, San Jose, CA) was added. Plates were incubated for another 4 h and then spun at 4 °C to remove the medium. Cells were resuspended in 40 µL of 1:200 diluted anti-CD8-PerCP-Cy5.5 (clone 53–6.7; BD Biosciences) and 1:400 diluted anti-CD4-PE-Cy7 (clone RM4-5; BD Biosciences) antibodies. After 30 min of incubation on ice, cells were washed, resuspended in 100 µL of Cytofix/Cytoperm solution, and incubated on ice for 20 min. After two washes, cells were stained with 40 µL of 1:200 diluted anti-IFN-γ APC antibody (clone XMG1.2; BD Biosciences) overnight at 4 °C. Cells were washed three times before acquisition using a FACS LSR II (Institute of Biomedical Sciences, Academia Sinica). Analysis was done by FlowJo software. Backgrounds as determined for samples without peptide stimulation were subtracted from the values presented for test samples.

MERS-CoV Neutralization Assay: The standard Vero E6 cell-based microneutralization assay was performed in an approved biosafety level 3 (BSL-3) laboratory to determine the titer of neutralizing antibodies against live MERS-CoV, as previously described.[54] Briefly, serially twofold diluted mouse sera were incubated with ≈100 infectious MERS-CoV (EMC-2012 strain) at room temperature for 2 h before transferring to confluent Vero E6 cells for cultivation at 37 °C incubator for 72 h. The neutralizing capability of the mouse sera was determined by the presence or absence of virus-induced cytopathic effect (CPE). Neutralizing antibody titers were expressed as the reciprocal of the highest dilution of sera that completely inhibited virus-induced CPE in 100% of the wells (NT_{100}).

MERS-CoV Challenge Studies: The MERS-CoV challenge studies were all conducted within approved BSL-3 and animal BSL-3 laboratories at the Galveston National Laboratory, strictly following approved notification-of-usage (NOU) and animal protocols and the guidelines and regulations of the National Institute of Health and AAALAC. For the proof-of-principle study, two groups of five age- and sex-matched human DPP4-transgenic mice were immunized subcutaneously twice, four weeks apart, with either the MERS-CoV RBD nanoparticle vaccine or control nanoparticles. The nanoparticles were thawed in a 37 °C water bath from samples that were stored at −20 °C for 2 months. Four weeks after the booster, mice were bled for assessing MERS-CoV RBD-specific IgG and neutralizing antibody responses prior to intranasal (i.n.) challenge with 100 LD_{50} (50% lethal dose) (≈10^3 $TCID_{50}$) of MERS-CoV (EMC/2012 strain). Virally challenged mice were monitored daily for clinical manifestations (i.e., weight loss) and mortality for at least 24 d after infection. Two of the five mice were sacrificed on day 2 postchallenge to assess the lung viral loads by Vero E6-based infection assay and quantitative PCR as previously described.[55] In addition, the lung tissues were processed, paraffin-embedded, and hematoxylin-and-eosin (H&E)-stained for assessing the histopathology, as previously described.[56]

Statistical Analyses: Data were analyzed by nonparametric unpaired *t* tests (Mann-Whitney) or ANOVA followed by Dunnett's multiple comparison tests using GraphPad Prism (GraphPad Software, San Diego, CA). The *p* values smaller than 0.05 were considered statistical significance.

Supporting Information

Supporting Information is available from the Wiley Online Library or from the author.

Acknowledgements

The authors acknowledge funding support by the Ministry of Science and Technology, Taiwan (105-2321-B-001-055, 106-2321-B-001-034, 107-2321-B-001-012, 106-2119-M-001-010, and 107-2119-M-001-042), Academia Sinica Career Development Award (AS-CDA-105-L06), Infectious Diseases Research and Education Center, and the National Taiwan University (107L104315).

Conflict of Interest

The authors declare no conflict of interest.

Keywords

cdGMP adjuvant, hollow nanoparticle, Middle East respiratory syndrome coronavirus, STING, virus mimicry

Received: October 29, 2018
Revised: March 17, 2019
Published online:

[1] L. C.-W. Lin, S. Chattopadhyay, J.-C. Lin, C.-M. J. Hu, *Adv. Healthcare Mater.* **2018**, *7*, 1701395.
[2] S. T. Reddy, A. J. van der Vlies, E. Simeoni, V. Angeli, G. J. Randolph, C. P. O'Neil, L. K. Lee, M. A. Swartz, J. A. Hubbell, *Nat. Biotechnol.* **2007**, *25*, 1159.
[3] C. A. Fromen, G. R. Robbins, T. W. Shen, M. P. Kai, J. P. Y. Ting, J. M. DeSimone, *Proc. Natl. Acad. Sci. USA* **2015**, *112*, 488.
[4] J. M. Blander, R. Medzhitov, *Nature* **2006**, *440*, 808.
[5] a) H. Ishikawa, Z. Ma, G. N. Barber, *Nature* **2009**, *461*, 788; b) L. Sun, J. Wu, F. Du, X. Chen, Z. J. Chen, *Science* **2013**, *339*, 786.
[6] a) D. L. Burdette, K. M. Monroe, K. Sotelo-Troha, J. S. Iwig, B. Eckert, M. Hyodo, Y. Hayakawa, R. E. Vance, *Nature* **2011**, *478*, 515; b) J. Wu, L. Sun, X. Chen, F. Du, H. Shi, C. Chen, Z. J. Chen, *Science* **2013**, *339*, 826.
[7] F. Guo, Y. Han, X. Zhao, J. Wang, F. Liu, C. Xu, L. Wei, J. D. Jiang, T. M. Block, J. T. Guo, J. Chang, *Antimicrob. Agents Chemother.* **2015**, *59*, 1273.
[8] J. Crouse, U. Kalinke, A. Oxenius, *Nat. Rev. Immunol.* **2015**, *15*, 231.
[9] a) M. C. Hanson, M. P. Crespo, W. Abraham, K. D. Moynihan, G. L. Szeto, S. H. Chen, M. B. Melo, S. Mueller, D. J. Irvine, *J. Clin. Invest.* **2015**, *125*, 2532; b) R. D. Junkins, M. D. Gallovic, B. M. Johnson, M. A. Collier, R. Watkins-Schulz, N. Cheng, C. N. David, C. E. McGee, G. D. Sempowski, I. Shterev, K. McKinnon, E. M. Bachelder, K. M. Ainslie, J. P.-Y. Ting, *J. Controlled Release* **2018**, *270*, 1; c) V. Neuhaus, J. A. Chichester, T. Ebensen, K. Schwarz, C. E. Hartman, Y. Shoji, C. A. Guzmán, V. Yusibov, K. Sewald, A. Braun, *Vaccine* **2014**, *32*, 3216.
[10] World Health Organization, *WHO MERS-CoV Global Summary and Assessment of Risk*, World Health Organization, Geneva, Switzerland **2018**.
[11] A. M. Zaki, S. van Boheemen, T. M. Bestebroer, A. D. M. E. Osterhaus, R. A. M. Fouchier, *N. Engl. J. Med.* **2012**, *367*, 1814.
[12] a) N. K. Alharbi, E. Padron-Regalado, C. P. Thompson, A. Kupke, D. Wells, M. A. Sloan, K. Grehan, N. Temperton, T. Lambe, G. Warimwe, S. Becker, A. V. S. Hill, S. C. Gilbert, *Vaccine* **2017**, *35*, 3780; b) B. L. Haagmans, J. M. A. van den Brand, V. S. Raj, A. Volz, P. Wohlsein, S. L. Smits, D. Schipper, T. M. Bestebroer, N. Okba, R. Fux, A. Bensaid, D. Solanes Foz, T. Kuiken, W. Baumgärtner, J. Segalés, G. Sutter, A. D. M. E. Osterhaus, *Science* **2016**, *351*, 77; c) E. Kim, K. Okada, T. Kenniston, V. S. Raj, M. M. AlHajri, E. A. B. A. Farag, F. AlHajri, A. D. M. E. Osterhaus, B. L. Haagmans, A. Gambotto, *Vaccine* **2014**, *32*, 5975; d) F. Song, R. Fux, L. B. Provacia, A. Volz, M. Eickmann, S. Becker, A. D. M. E. Osterhaus, B. L. Haagmans, G. Sutter, *J. Virol.* **2013**, *87*, 11950; e) A. Volz, A. Kupke, F. Song, S. Jany, R. Fux, H. Shams-Eldin, J. Schmidt, C. Becker, M. Eickmann, S. Becker, G. Sutter, *J. Virol.* **2015**, *89*, 8651; f) X. Guo, Y. Deng, H. Chen, J. Lan, W. Wang, X. Zou, T. Hung, Z. Lu, W. Tan, *Immunology* **2015**, *145*, 476.
[13] a) C. Ma, Y. Li, L. Wang, G. Zhao, X. Tao, C. T. K. Tseng, Y. Zhou, L. Du, S. Jiang, *Vaccine* **2014**, *32*, 2100; b) J. Tang, N. Zhang, X. Tao, G. Zhao, Y. Guo, C. T. K. Tseng, S. Jiang, L. Du, Y. Zhou, *Hum. Vaccines Immunother.* **2015**, *11*, 1244; c) C. M. Coleman, Y. V. Liu, H. Mu, J. K. Taylor, M. Massare, D. C. Flyer, G. M. Glenn, G. E. Smith, M. B. Frieman, *Vaccine* **2014**, *32*, 3169; d) C. M. Coleman, T. Venkataraman, Y. V. Liu, G. M. Glenn, G. E. Smith, D. C. Flyer, M. B. Frieman, *Vaccine* **2017**, *35*, 1586; e) J. Lan, Y. Deng, H. Chen, G. Lu, W. Wang, X. Guo, Z. Lu, G. F. Gao, W. Tan, *PLoS One* **2014**, *9*, 1; f) N. Zhang, R. Channappanavar, C. Ma, L. Wang, J. Tang, T. Garron, X. Tao, S. Tasneem, L. Lu, C.-T. K. Tseng, Y. Zhou, S. Perlman, S. Jiang, L. Du, *Cell Mol. Immunol.* **2016**, *13*, 180; g) J. Lan, Y. Yao, Y. Deng, H. Chen, G. Lu, W. Wang, L. Bao, W. Deng, Q. Wei, G. F. Gao, C. Qin, W. Tan, *EBioMed.* **2015**, *2*, 1438.
[14] A. S. Agrawal, X. Tao, A. Algaissi, T. Garron, K. Narayanan, B. H. Peng, R. B. Couch, C. K. Tseng, *Hum Vaccines Immunother.* **2016**, https://doi.org/10.1080/21645515.2016.11776881.
[15] a) J. Zhao, A. N. Alshukairi, S. A. Baharoon, W. A. Ahmed, A. A. Bokhari, A. M. Nehdi, L. A. Layqah, M. G. Alghamdi, M. M. Al Gethamy, A. M. Dada, I. Khalid, M. Boujelal, S. M. Al Johani, L. Vogel, K. Subbarao, A. Mangalam, C. Wu, P. Ten Eyck, S. Perlman, J. Zhao, *Sci. Immunol.* **2017**, *2*, eaan5393; b) R. Channappanavar, J. Zhao, S. Perlman, *Immunol. Res.* **2014**, *59*, 118.
[16] B. M. Discher, Y. Y. Won, D. S. Ege, J. C. Lee, F. S. Bates, D. E. Discher, D. A. Hammer, *Science* **1999**, *284*, 1143.
[17] H. Qi, H. Zhou, Q. Tang, J. Y. Lee, Z. Fan, S. Kim, M. C. Staub, T. Zhou, S. Mei, L. Han, D. J. Pochan, H. Cheng, W. Hu, C. Y. Li, *Nat. Commun.* **2018**, *9*, 3005.
[18] S. Colombo, D. Cun, K. Remaut, M. Bunker, J. Zhang, B. Martin-Bertelsen, A. Yaghmur, L. Braeckmans, H. M. Nielsen, C. Foged, *J. Controlled Release* **2015**, *201*, 22.
[19] N. M. Pinkerton, A. Grandeury, A. Fisch, J. Brozio, B. U. Riebesehl, R. K. Prud'homme, *Mol. Pharmaceutics* **2013**, *10*, 319.
[20] H. Schonhorn, *J. Chem. Eng. Data* **1967**, *12*, 524.
[21] a) P. Banerjee, A. Biswas, T. Biswas, *Int. Immunol.* **2008**, *20*, 1551; b) S. R. Crowe, S. J. Turner, S. C. Miller, A. D. Roberts, R. a. Rappolo, P. C. Doherty, K. H. Ely, D. L. Woodland, *J. Exp. Med.* **2003**, *198*, 399; c) L. Deng, T. Z. Chang, Y. Wang, S. Li, S. Wang, S. Matsuyama, G. Yu, R. W. Compans, J. D. Li, M. R. Prausnitz, J. A. Champion, B. Z. Wang, *Proc. Natl. Acad. Sci. USA* **2018**, *115*, E7758; d) M. C. Gold, M. W. Munks, M. Wagner, U. H. Koszinowski, A. B. Hill, S. P. Fling, *J. Immunol.* **2002**, *169*, 359; e) Y. Ye, C. Wang, X. Zhang, Q. Hu, Y. Zhang, Q. Liu, D. Wen, J. Milligan, A. Bellotti, L. Huang, G. Dotti, Z. Gu, *Sci. Immunol.* **2017**, *2*, eaan5692.
[22] a) X. Jiang, C. Shen, J. Rey-Ladino, H. Yu, R. C. Brunham, *Infect. Immun.* **2008**, *76*, 2392; b) J. M. Silva, G. Vandermeulen, V. G. Oliveira, S. N. Pinto, C. Rodrigues, A. Salgado, C. A. Afonso, A. S. Viana, C. Jérôme, L. C. Silva, L. Graca, V. Préat, H. F. Florindo, *Nanomedicine* **2014**, *9*, 2639.
[23] T. Junt, E. A. Moseman, M. Iannacone, S. Massberg, P. A. Lang, M. Boes, K. Fink, S. E. Henrickson, D. M. Shayakhmetov, N. C. Di Paolo, N. Van Rooijen, T. R. Mempel, S. P. Whelan, U. H. von Andrian, *Nature* **2007**, *450*, 110.
[24] a) S. F. Gonzalez, V. Lukacs-Kornek, M. P. Kuligowski, L. A. Pitcher, S. E. Degn, Y. A. Kim, M. J. Cloninger, L. Martinez-Pomares, S. Gordon, S. J. Turley, M. C. Carroll, *Nat. Immunol.* **2010**, *11*, 427;

b) C. C. Norbury, D. Malide, J. S. Gibbs, J. R. Bennink, J. W. Yewdell, *Nat. Immunol.* **2002**, *3*, 265.
[25] S. M. Kaech, W. Cui, *Nat. Rev. Immunol.* **2012**, *12*, 749.
[26] a) W. J. Liu, M. Zhao, K. Liu, K. Xu, G. Wong, W. Tan, G. F. Gao, *Antiviral Res.* **2017**, *137*, 82; b) W. J. Liu, J. Lan, K. Liu, Y. Deng, Y. Yao, S. Wu, H. Chen, L. Bao, H. Zhang, M. Zhao, Q. Wang, L. Han, Y. Chai, J. Qi, J. Zhao, S. Meng, C. Qin, G. F. Gao, W. Tan, *J. Immunol.* **2017**, *198*, 873.
[27] J. Zhao, K. Li, C. Wohlford-Lenane, S. S. Agnihothram, C. Fett, J. Zhao, M. J. Gale, R. S. Baric, L. Enjuanes, T. Gallagher, P. B. McCray, S. Perlman, *Proc. Natl. Acad. Sci. USA* **2014**, *111*, 4970.
[28] a) M. Bolles, D. Deming, K. Long, S. Agnihothram, A. Whitmore, M. Ferris, W. Funkhouser, L. Gralinski, A. Totura, M. Heise, R. S. Baric, *J. Virol.* **2011**, *85*, 12201; b) C. T. Tseng, E. Sbrana, N. Iwata-Yoshikawa, P. C. Newman, T. Garron, R. L. Atmar, C. J. Peters, R. B. Couch, *PLoS One* **2012**, *7*, e35421; c) H. Weingartl, M. Czub, S. Czub, J. Neufeld, P. Marszal, J. Gren, G. Smith, S. Jones, R. Proulx, Y. Deschambault, E. Grudeski, A. Andonov, R. He, Y. Li, J. Copps, A. Grolla, D. Dick, J. Berry, S. Ganske, L. Manning, J. Cao, *J. Virol.* **2004**, *78*, 12672; d) A. S. Agrawal, X. Tao, A. Algaissi, T. Garron, K. Narayanan, B. H. Peng, R. B. Couch, C. T. Tseng, *Hum Vaccines Immunother.* **2016**, *12*, 2351.
[29] Y. Honda-Okubo, D. Barnard, C. H. Ong, B. H. Peng, C. T. K. Tseng, N. Petrovsky, *J. Virol.* **2015**, *89*, 2995.
[30] J. Zhao, J. Zhao, A. K. Mangalam, R. Channappanavar, C. Fett, D. K. Meyerholz, S. Agnihothram, R. S. Baric, C. S. David, S. Perlman, *Immunity* **2016**, *44*, 1379.
[31] K. Muthumani, D. Falzarano, E. L. Reuschel, C. Tingey, S. Flingai, D. O. Villarreal, M. Wise, A. Patel, A. Izmirly, A. Aljuaid, A. M. Seliga, G. Soule, M. Morrow, K. A. Kraynyak, A. S. Khan, D. P. Scott, F. Feldmann, R. LaCasse, K. Meade-White, A. Okumura, K. E. Ugen, N. Y. Sardesai, J. J. Kim, G. Kobinger, H. Feldmann, D. B. Weiner, *Sci. Transl. Med.* **2015**, *7*, 301ra132.
[32] B. L. Haagmans, J. M. A. van den Brand, V. S. Raj, A. Volz, P. Wohlsein, S. L. Smits, D. Schipper, T. M. Bestebroer, N. Okba, R. Fux, A. Bensaid, D. S. Foz, T. Kuiken, W. Baumgartner, J. Segales, G. Sutter, A. D. M. E. Osterhaus, *Science* **2016**, *351*, 77.
[33] L. S. Wang, W. Shi, J. D. Chappell, M. G. Joyce, Y. Zhang, M. Kanekiyo, M. M. Becker, N. van Doremalen, R. Fischer, N. S. Wang, K. S. Corbett, M. Choe, R. D. Mason, J. G. Van Galen, T. Q. Zhou, K. O. Saunders, K. M. Tatti, L. M. Haynes, P. D. Kwong, K. Modjarrad, W. P. Kong, J. S. McLellan, M. R. Denison, V. J. Munster, J. R. Mascola, B. S. Graham, *Virol. J.* **2018**, *15*, 92.
[34] b) L. Du, Z. Kou, C. Ma, X. Tao, L. Wang, G. Zhao, Y. Chen, F. Yu, C. T. Tseng, Y. Zhou, S. Jiang, *PLoS One* **2013**, *8*, e81587.
[35] b) L. Nuhn, N. Vanparijs, A. De Beuckelaer, L. Lybaert, G. Verstraete, K. Deswarte, S. Lienenklaus, N. M. Shukla, A. C. Salyer, B. N. Lambrecht, J. Grooten, S. A. David, S. De Koker, B. G. De Geest, *Proc. Natl. Acad. Sci. USA* **2016**, *113*, 8098; c) P. O. Ilyinskii, C. J. Roy, C. P. O'Neil, E. A. Browning, L. A. Pittet, D. H. Altreuter, F. Alexis, E. Tonti, J. Shi, P. A. Basto, M. Iannacone, A. F. Radovic-Moreno, R. S. Langer, O. C. Farokhzad, U. H. von Andrian, L. P. M. Johnston, T. K. Kishimoto, *Vaccine* **2014**, *32*, 2882; d) G. M. Lynn, R. Laga, P. A. Darrah, A. S. Ishizuka, A. J. Balaci, A. E. Dulcey, M. Pechar, R. Pola, M. Y. Gerner, A. Yamamoto, C. R. Buechler, K. M. Quinn, M. G. Smelkinson, O. Vanek, R. Cawood, T. Hills, O. Vasalatiy, K. Kastenmüller, J. R. Francica, L. Stutts, J. K. Tom, K. A. Ryu, A. P. Esser-Kahn, T. Etrych, K. D. Fisher, L. W. Seymour, R. A. Seder, *Nat. Biotechnol.* **2015**, *33*, 1201.
[36] S. T. Koshy, A. S. Cheung, L. Gu, A. R. Graveline, D. J. Mooney, *Adv. Biosyst.* **2017**, *1*, 1600013.
[37] T. J. Goodwin, L. Huang, *Vaccine* **2017**, *35*, 2550.
[38] a) R. D. Junkins, M. D. Gallovic, B. M. Johnson, M. A. Collier, R. Watkins-Schulz, N. Cheng, C. N. David, C. E. McGee, G. D. Sempowski, I. Shterev, K. McKinnon, E. M. Bachelder, K. M. Ainslie, J. P. Ting, *J Control Release* **2018**, *270*, 1; b) M. A. Collier, R. D. Junkins, M. D. Gallovic, B. M. Johnson, M. M. Johnson, A. N. Macintyre, G. D. Sempowski, E. M. Bachelder, J. P. Y. Ting, K. M. Ainslie, *Mol. Pharmaceutics* **2018**, *15*, 4933.
[39] a) D. R. Wilson, R. Sen, J. C. Sunshine, D. M. Pardoll, J. J. Green, Y. J. Kim, *Nanomedicine* **2018**, *14*, 237; b) C. Aroh, Z. H. Wang, N. Dobbs, M. Luo, Z. J. Chen, J. M. Gao, N. Yan, *J. Immunol.* **2017**, *199*, 3840.
[40] S. Chattopadhyay, J. Y. Chen, H. W. Chen, C. J. Hu, *Nanotheranostics* **2017**, *1*, 244.
[41] a) B. Fallet, K. Narr, Y. I. Ertuna, M. Remy, R. Sommerstein, K. Cornille, M. Kreutzfeldt, N. Page, G. Zimmer, F. Geier, T. Straub, H. Pircher, K. Larimore, P. D. Greenberg, D. Merkler, D. D. Pinschewer, *Sci. Immunol.* **2016**, *1*, 6817; b) C. A. Segura-Cerda, M. J. Aceves-Sanchez, B. Marquina-Castillo, D. Mata-Espinoza, J. Barrios-Payan, P. J. Vega-Dominguez, C. Pedroza-Roldan, J. Bravo-Madrigal, A. A. Vallejo-Cardona, R. Hernandez-Pando, M. A. Flores-Valdez, *Vaccine* **2018**, *36*, 2069.
[42] A. Tzeng, M. J. Kauke, E. F. Zhu, K. D. Moynihan, C. F. Opel, N. J. Yang, N. Mehta, R. L. Kelly, G. L. Szeto, W. W. Overwijk, D. J. Irvine, K. D. Wittrup, *Cell Rep.* **2016**, *17*, 2503.
[43] K. E. Sivick, A. L. Desbien, L. H. Glickman, G. L. Reiner, L. Corrales, N. H. Surh, T. E. Hudson, U. T. Vu, B. J. Francica, T. Banda, G. E. Katibah, D. B. Kanne, J. J. Leong, K. Metchette, J. R. Bruml, C. O. Ndubaku, J. M. McKenna, Y. Feng, L. X. Zheng, S. L. Bender, C. Y. Cho, M. L. Leong, A. van Elsas, T. W. Dubensky, S. M. McWhirter, *Cell Rep.* **2018**, *25*, 3074.
[44] a) G. M. Boxx, G. Cheng, *Cell Host Microbe* **2016**, *19*, 760; b) S. a. Stifter, C. G. Feng, *J. Immunol.* **2015**, *194*, 2455; c) L. Moreira-Teixeira, K. Mayer-Barber, A. Sher, A. O'Garra, *J. Exp. Med.* **2018**, *215*, 1273.
[45] a) X.-D. Li, J. Wu, D. Gao, H. Wang, L. Sun, Z. J. Chen, *Science* **2013**, *341*, 1390; b) L. Moreira-Teixeira, K. Mayer-Barber, A. Sher, A. O'Garra, *J. Exp. Med.* **2018**, *215*, 1273.
[46] a) L. S. Wang, W. Shi, M. G. Joyce, K. Modjarrad, Y. Zhang, K. Leung, C. R. Lees, T. Q. Zhou, H. M. Yassine, M. Kanekiyo, Z. Y. Yang, X. J. Chen, M. M. Becker, M. Freeman, L. Vogel, J. C. Johnson, G. Olinger, J. P. Todd, U. Bagci, J. Solomon, D. J. Mollura, L. Hensley, P. Jahrling, M. R. Denison, S. S. Rao, K. Subbarao, P. D. Kwong, J. R. Mascola, W. P. Kong, B. S. Graham, *Nat. Commun.* **2015**, *6*, 7712; b) C. Q. Ma, L. L. Wang, X. R. Tao, N. R. Zhang, Y. Yang, C. T. K. Tseng, F. Li, Y. S. Zhou, S. B. Jiang, L. Y. Du, *Vaccine* **2014**, *32*, 6170; c) C. M. Coleman, Y. V. Liu, H. Y. Mu, J. K. Taylor, M. Massare, D. C. Flyer, G. M. Glenn, G. E. Smith, M. B. Frieman, *Vaccine* **2014**, *32*, 3169.
[47] K. V. Houser, A. J. Broadbent, L. Gretebeck, L. Vogel, E. W. Lamirande, T. Sutton, K. W. Bock, M. Minai, M. Orandle, I. N. Moore, K. Subbarao, *PLoS Pathog.* **2017**, *13*, e1006565.
[48] A. M. Hashem, A. Algaissi, A. Agrawal, S. S. Al-Amri, R. Y. Alhabbab, S. S. Sohrab, A. Almasoud, N. K. Alharbi, B. H. Peng, M. Russell, X. Li, C. T. K. Tseng, *J. Infect. Dis.* **2019**, https://doi.org/ 10.1093/infdis/jiz137.
[49] a) D. J. Irvine, M. A. Swartz, G. L. Szeto, *Nat. Mater.* **2013**, *12*, 978; b) M. Tamborrini, N. Geib, A. Marrero-Nodarse, M. Jud, J. Hauser, C. Aho, A. Lamelas, A. Zuniga, G. Pluschke, A. Ghasparian, J. A. Robinson, *Vaccines* **2015**, *3*, 850.
[50] a) J. Hrkach, D. Von Hoff, M. Mukkaram Ali, E. Andrianova, J. Auer, T. Campbell, D. De Witt, M. Figa, M. Figueiredo, A. Horhota, S. Low, K. McDonnell, E. Peeke, B. Retnarajan, A. Sabnis, E. Schnipper, J. J. Song, Y. H. Song, J. Summa, D. Tompsett, G. Troiano, T. Van Geen Hoven, J. Wright, P. LoRusso, P. W. Kantoff, N. H. Bander, C. Sweeney, O. C. Farokhzad, R. Langer, S. Zale, *Sci. Transl. Med.* **2012**, *4*, 128ra39; b) A. L. Galloway, A. Murphy, J. M. DeSimone, J. Di, J. P. Herrmann, M. E. Hunter, J. P. Kindig,

F. J. Malinoski, M. A. Rumley, D. M. Stoltz, T. S. Templeman, B. Hubby, *Nanomedicine* **2013**, *9*, 523; c) E. A. Thompson, S. Ols, K. Miura, K. Rausch, D. L. Narum, M. Spangberg, M. Juraska, U. Wille-Reece, A. Weiner, R. F. Howard, C. A. Long, P. E. Duffy, L. Johnston, C. P. O'Neil, K. Lore, *JCI Insight* **2018**, *3*, 120692.

[51] A. S. Agrawal, T. Garron, X. Tao, B.-H. Peng, M. Wakamiya, T.-S. Chan, R. B. Couch, C.-T. K. Tseng, *J. Virol.* **2015**, *89*, 3659.

[52] a) A. B. Roy, O. E. Petrova, K. Sauer, *Bio-Protocol* **2013**, *3*, e828; b) C. Spangler, A. Böhm, U. Jenal, R. Seifert, V. Kaever, *J. Microbiol. Methods* **2010**, *81*, 226.

[53] M. P. Matheu, D. Sen, M. D. Cahalan, I. Parker, *J. Visualized Exp.* **2008**, *9*, 773.

[54] X. Tao, T. Garron, A. S. Agrawal, A. Algaissi, B. H. Peng, M. Wakamiya, T. S. Chan, L. Lu, L. Du, S. Jiang, R. B. Couch, C. T. Tseng, *J. Virol.* **2016**, *90*, 57.

[55] M. P. Nyon, L. Du, C. K. Tseng, C. A. Seid, J. Pollet, K. S. Naceanceno, A. Agrawal, A. Algaissi, B. H. Peng, W. Tai, S. Jiang, M. E. Bottazzi, U. Strych, P. J. Hotez, *Vaccine* **2018**, *36*, 1853.

[56] A. S. Agrawal, T. Garron, X. Tao, B. H. Peng, M. Wakamiya, T. S. Chan, R. B. Couch, C. T. Tseng, *J. Virol.* **2015**, *89*, 3659.